Novel Role for the *Streptococcus pneumoniae* Toxin Pneumolysin in the Assembly of Biofilms

Joshua R. Shak,[a] Herbert P. Ludewick,[a,b] Kristen E. Howery,[a] Fuminori Sakai,[a] Hong Yi,[c] Richard M. Harvey,[d] James C. Paton,[d] Keith P. Klugman,[a] Jorge E. Vidal[a]

Hubert Department of Global Health, Rollins School of Public Health, Emory University, Atlanta, Georgia, USA[a]; Center for Immunology & Microbial Disease, Albany Medical College, Albany, New York, USA[b]; Robert P. Apkarian Integrated Electron Microscopy Core, Emory University, Atlanta, Georgia, USA[c];Research Centre for Infectious Diseases, School of Molecular and Biomedical Science, University of Adelaide, Adelaide, Australia[d]

J.R.S. and H.P.L. contributed equally to this article.

ABSTRACT ***Streptococcus pneumoniae* is an important commensal and pathogen responsible for almost a million deaths annually in children under five. The formation of biofilms by *S. pneumoniae* is important in nasopharyngeal colonization, pneumonia, and otitis media. Pneumolysin (Ply) is a toxin that contributes significantly to the virulence of *S. pneumoniae* and is an important candidate as a serotype-independent vaccine target. Having previously demonstrated that a *luxS* knockout mutant was unable to form early biofilms and expressed less *ply* mRNA than the wild type, we conducted a study to investigate the role of Ply in biofilm formation. We found that Ply was expressed in early phases of biofilm development and localized to cellular aggregates as early as 4 h postinoculation. *S. pneumoniae ply* knockout mutants in D39 and TIGR4 backgrounds produced significantly less biofilm biomass than wild-type strains at early time points, both on polystyrene and on human respiratory epithelial cells, cultured under static or continuous-flow conditions. Ply's role in biofilm formation appears to be independent of its hemolytic activity, as *S. pneumoniae* serotype 1 strains, which produce a nonhemolytic variant of Ply, were still able to form biofilms. Transmission electron microscopy of biofilms grown on A549 lung cells using immunogold demonstrated that Ply was located both on the surfaces of pneumococcal cells and in the extracellular biofilm matrix. Altogether, our studies demonstrate a novel role for pneumolysin in the assembly of *S. pneumoniae* biofilms that is likely important during both carriage and disease and therefore significant for pneumolysin-targeting vaccines under development.**

IMPORTANCE **The bacterium *Streptococcus pneumoniae* (commonly known as the pneumococcus) is commonly carried in the human nasopharynx and can spread to other body sites to cause disease. In the nasopharynx, middle ear, and lungs, the pneumococcus forms multicellular surface-associated structures called biofilms. Pneumolysin is an important toxin produced by almost all *S. pneumoniae* strains, extensively studied for its ability to cause damage to human tissue. In this paper, we demonstrate that pneumolysin has a previously unrecognized role in biofilm formation by showing that strains without pneumolysin are unable to form the same amount of biofilm on plastic and human cell substrates. Furthermore, we show that the role of pneumolysin in biofilm formation is separate from the hemolytic activity responsible for tissue damage during pneumococcal diseases. This novel role for pneumolysin suggests that pneumococcal vaccines directed against this protein should be investigated for their potential impact on biofilms formed during carriage and disease.**

Received 10 August 2013 **Accepted** 21 August 2013 **Published** 10 September 2013

Citation Shak JR, Ludewick HP, Howery KE, Sakai F, Yi H, Harvey RM, Paton JC, Klugman KP, Vidal JE. 2013. Novel role for the *Streptococcus pneumoniae* toxin pneumolysin in the assembly of biofilms. mBio 4(5):e00655-13. doi:10.1128/mBio.00655-13.

Editor Larry McDaniel, University of Mississippi Medical Center

Address correspondence to Jorge E. Vidal, jvidalg@emory.edu.

Streptococcus pneumoniae (the pneumococcus) is a Gram-positive bacterium annually responsible for 14.5 million cases of disease and 800,000 deaths in children under 5 years of age (1). The pneumococcus colonizes the nasopharynx in up to 90% of children and approximately 15% of adults and can spread from there to other anatomic sites to cause sinusitis, otitis media, pneumonia, bacteremia, and meningitis (2). Biofilm formation is important, both for colonization of the human nasopharynx and in pathogenesis (3). In particular, the role of pneumococcal biofilms in otitis media has been clearly demonstrated in humans (4) and investigated in a chinchilla model (5, 6). Despite the relevance of biofilms in commensalism and pathogenesis, the mechanisms of pneumococcal biofilm formation are not yet fully understood. Our laboratories have previously demonstrated that LuxS, the autoinducer 2 (AI-2) synthase, is essential for biofilm formation at early time points (7, 8) and observed that transcription of *ply*, the gene that encodes pneumolysin, is down-regulated approximately 35-fold in a *luxS*-null mutant (7).

Pneumolysin (Ply) is a well-established virulence factor (9, 10) that has been extensively studied for its hemolytic activity and cytotoxic properties. Ply, a 53-kDa surface protein (11), is a cholesterol-dependent cytolysin that binds cholesterol in eukary-

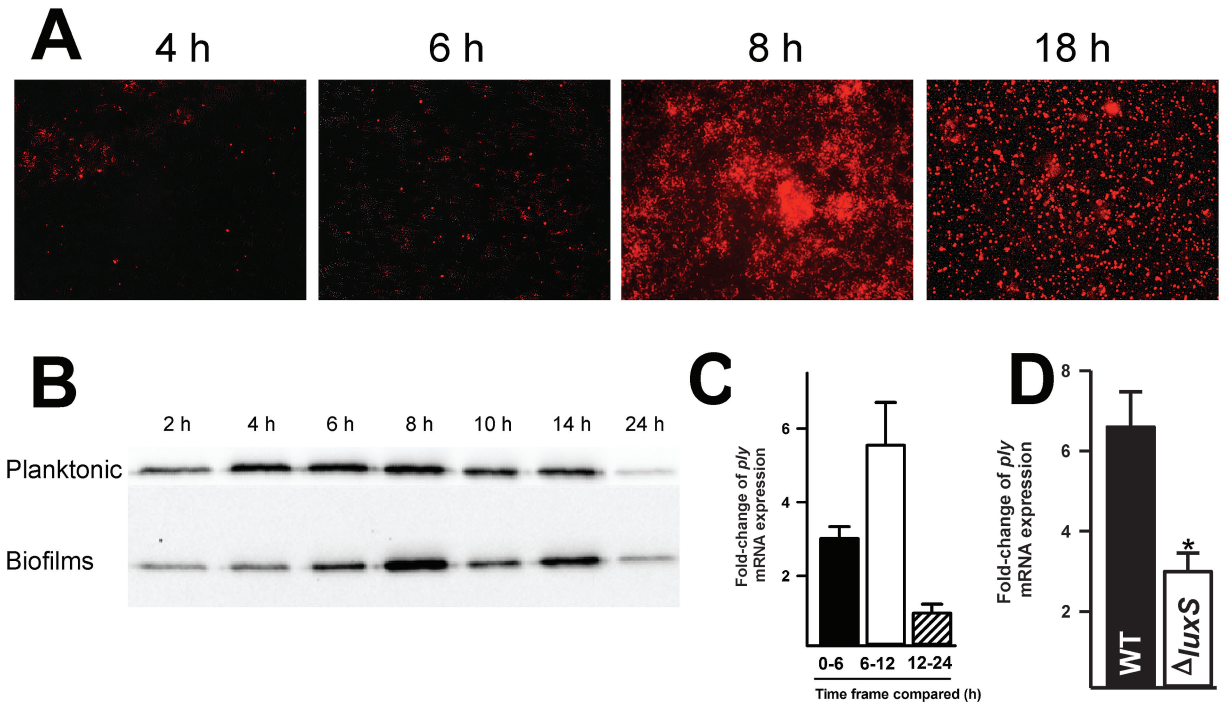

FIG 1 Pneumolysin is expressed in *S. pneumoniae* biofilms. (A) Fluorescence microscopy of wild-type D39 biofilms visualized with an anti-Ply antibody and a secondary conjugated antibody demonstrates Ply expression at 4, 6, 8, and 18 h. (B) Cell lysates from wild-type D39 grown in planktonic cultures or biofilms grown on polystyrene plates were probed by Western blotting. (C) To examine pneumolysin expression over time qPCR of cDNA was used to compare levels of *ply* mRNA at different time points of biofilm formation on polystyrene. Levels of *ply* mRNA were compared between the inoculum (0 h) and the 6-h biofilm, between 6-h and 12-h biofilms, and between 12-h and 24-h biofilms. (D) qPCR comparing levels of mRNA in 6-h biofilms to 12-h biofilms, showing that those formed by wild-type D39 have significantly more *ply* mRNA than those formed by D39Δ*luxS*. Error bars indicate standard errors of the means, and the asterisk indicates a *P* value of 0.01.

otic cell membranes and forms 400-Å pores that lead to cell lysis (12). Through its activity at the bacterial cell surface, or upon release through pneumococcal autolysis, Ply is responsible for almost all pneumococcal hemolytic activity (13). As anti-Ply antibodies are generated following carriage or otitis media (14–16) and TLR4-mediated recognition of pneumolysin stimulates a profound immune response (17, 18), a detoxified derivative of pneumolysin is under investigation as a serotype-independent vaccine candidate (19–21). However, it is currently unclear what role Ply plays during asymptomatic carriage that exposes this protein to the host immune system.

Though prior studies have demonstrated that the hemolytic alpha-toxin of *Staphylococcus aureus* is essential for biofilm formation on plastic and *ex vivo* porcine mucosa (22, 23), we are unaware of any other hemolysins being directly implicated in biofilm formation. That said, some preliminary data suggest that Ply has a role in pneumococcal biofilm development. A study of *S. pneumoniae* ATCC 6303 biofilms in a continuous-flow system demonstrated more Ply present in 3-day-old biofilms than in planktonic cultures (24), and more recently, Marks et al. reported that 48-h biofilms formed by a Ply-deficient mutant, grown on NCI-H292 epithelial cells with medium replacement every 12 hours, differed in appearance and biomass from wild-type D39 (25). Furthermore, our previous study of the role of LuxS/AI-2 in biofilm development suggests that genes regulated by LuxS, including *ply* (7, 26), the putative hemolysin SP1466 (26), and the *cbpD* gene, encoding choline-binding protein D (CbpD), may be important in biofilm development. While it has been shown that CbpD is required for biofilm formation (8), the role of pneumolysin in biofilm development has not been thoroughly investigated.

To assess whether Ply has a part in pneumococcal biofilm formation, we examined the timing and distribution of Ply expression in pneumococcal biofilms and evaluated biofilm formation of Ply knockout mutants under static and continuous-flow conditions, on both abiotic and human cell substrates. We found that Ply is expressed in pneumococcal biofilms, localizing to the earliest aggregates of cells, and knockout mutants deficient in Ply are impaired in their ability to form biofilms. While biofilm formation appears to mask the hemolytic activity of pneumococcal cells, pneumolysin's role in biofilm formation appears to be separate from its hemolytic activity. Altogether, our results demonstrate a novel and important role for Ply in the early development of pneumococcal biofilms.

RESULTS

Pneumolysin is expressed in pneumococcal biofilms. We first examined whether Ply was expressed in wild-type D39 during biofilm development in static cultures on a polystyrene substrate. To visualize Ply in biofilms, we employed a mouse monoclonal anti-Ply antibody followed by a fluorescently labeled anti-mouse antibody. Immunofluorescence images revealed low levels of Ply expression in biofilms 4 h and 6 h postinoculation, followed by maximal expression 8 h postinoculation and decreased expression

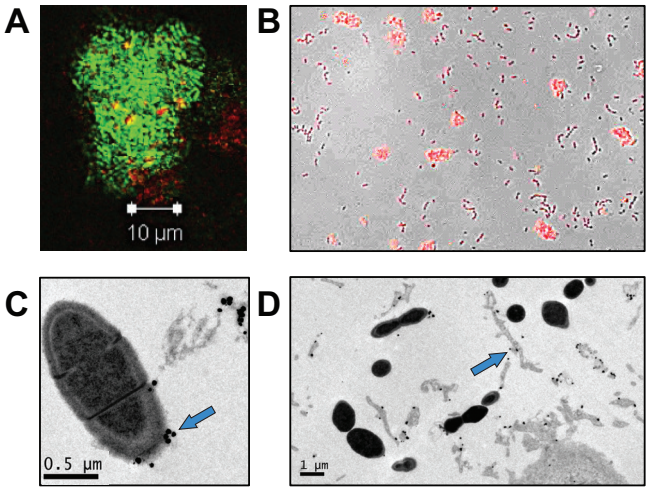

FIG 2 Location of pneumolysin in pneumococcal biofilms. (A) Confocal microscopy images of D39 (antipneumococcal antibody, green) and Ply (anti-Ply antibody, red) indicate that pneumococcal cells and pneumolysin colocalized in D39 biofilms at 24 h. (B) An image of differential interference contrast (Nomarski) with a fluorescent anti-Ply overlay of 4-h wild-type D39 biofilms revealed that pneumolysin localized to the earliest cellular aggregates in biofilms grown on polystyrene. (C) Transmission electron microscopy of an 8-h biofilm grown on A549 cells and treated with anti-Ply primary antibody and a gold-conjugated secondary antibody reveals that Ply is located on the bacterial surface (arrow) and in the extracellular matrix. (D) Another TEM image demonstrates Ply located throughout the extracellular matrix (arrow) between pneumococcal biofilm cells.

by 18 h (Fig. 1A). As a control, we probed 18-h biofilms of a *ply* knockout mutant (see Fig. S1 in the supplemental material) with the anti-Ply antibody and observed minimal fluorescence (see Fig. S2 in the supplemental material). Western blotting confirmed that pneumolysin is present in both planktonic and biofilm cells as early as 2 h postinoculation and reaches maximal expression 6 to 8 h following inoculation (Fig. 1B). Using reverse transcriptase and qPCR to quantify pneumolysin mRNA in biofilm cells, we found that *ply* expression increased from 0 to 6 h and from 6 to 12 h but there was little change in mRNA levels between 12 and 24 h (Fig. 1C). In line with our previous finding that *ply* is downregulated in planktonic cultures of D39Δ*luxS* (7), we found that the change in *ply* expression between 6 and 12 h in biofilms formed by D39Δ*luxS* was significantly less than in biofilms formed by wild-type D39 (Fig. 1D).

Pneumolysin localizes to cellular aggregates and is present in the cell wall and extracellular matrix. Using confocal microscopy to examine the location of Ply in three dimensions using an anti-Ply antibody and green fluorescent protein (GFP)-expressing wild-type D39 biofilms, we found that Ply colocalized with aggregates of biofilm cells (Fig. 2A). To confirm that the pneumolysin signal was specific to aggregates and not simply coincidental with the largest mass of cells, we examined sparse 4-h biofilms. Using differential interference contrast (Nomarski) images overlaid with images obtained using an anti-Ply antibody and a fluorescently labeled secondary antibody, we found that the Ply signal localized to nascent biofilm structures (i.e., early bacterial aggregates) (Fig. 2B). We then used immunogold transmission electron microscopy (TEM) to better localize Ply within 8-h biofilm structures and found that Ply localized to the bacterial cell well (arrow, Fig. 2C) and to the extracellular matrix (arrow, Fig. 2D). Altogether, these results confirm the specific localization of Ply to cellular aggregates and suggest a role as a matrix protein.

Early biofilm assembly on polystyrene is impaired in a Ply-deficient knockout. To examine whether Ply is essential for assembly of pneumococcal biofilms, we constructed a Ply-deficient knockout in D39 (see Fig. S1 in the supplemental material) and examined the biofilm formation of this mutant as well as a TIGR4 derivative provided by Andrew Camilli (Table 1). While the planktonic growth of the Ply-deficient mutants did not differ from that of the corresponding wild-type strains (see Fig. S3 in the supplemental material), the ability of the Δ*ply* derivatives to form biofilms was drastically impaired. Fluorescence microscopy of GFP-expressing derivatives of D39, D39Δ*ply*, AC2394 (TIGR4), and AC4037 (TIGR4Δ*ply*) demonstrated that biofilm formation ability of the Δ*ply* mutants was inferior to that of the wild-type

TABLE 1 Strains and plasmids used in this study

Strain or plasmid	Description	Reference or source
S. pneumoniae strains		
D39	Avery strain, clinical isolate, capsular serotype 2	46
SPJV01	D39/pMV158GFP, Tet^r	7
SPJV05	D39Δ*luxS* Ery^r	7
SPJV08	D39Δ*luxS*/pMV158GFP Ery^r Tet^r	7
SPJV10	D39Δ*comC* Ery^r	27
SPJV14	D39Δ*ply* Ery^r	This study
SPJV15	D39Δ*ply*/pMV158GFP Ery^r Tet^r	This study
Pn+	Reconstituted ply mutant	13
Ply306	D39 with ST 306 *ply* allele	This study
AC2394	Acapsular TIGR4, invasive clinical isolate	47
AC2394gfp	AC2394/pMV158GFP Tet^r	This study
AC4037	AC2394Δ*ply* Spc^r	47
AC4037gfp	AC2394Δ*ply*/pMV158GFP Spc^r Tet^r	This study
CDC_881	Serotype 1 strain, ST306	L. McGee, CDC
CDC_1403	Serotype 1 strain, ST306	L. McGee, CDC
CDC_4829	Serotype 1 strain, ST306	L. McGee, CDC
Plasmid		
pMV158GFP	*S. pneumoniae* mobilizable plasmid encoding GFP; confers resistance to tetracycline	48

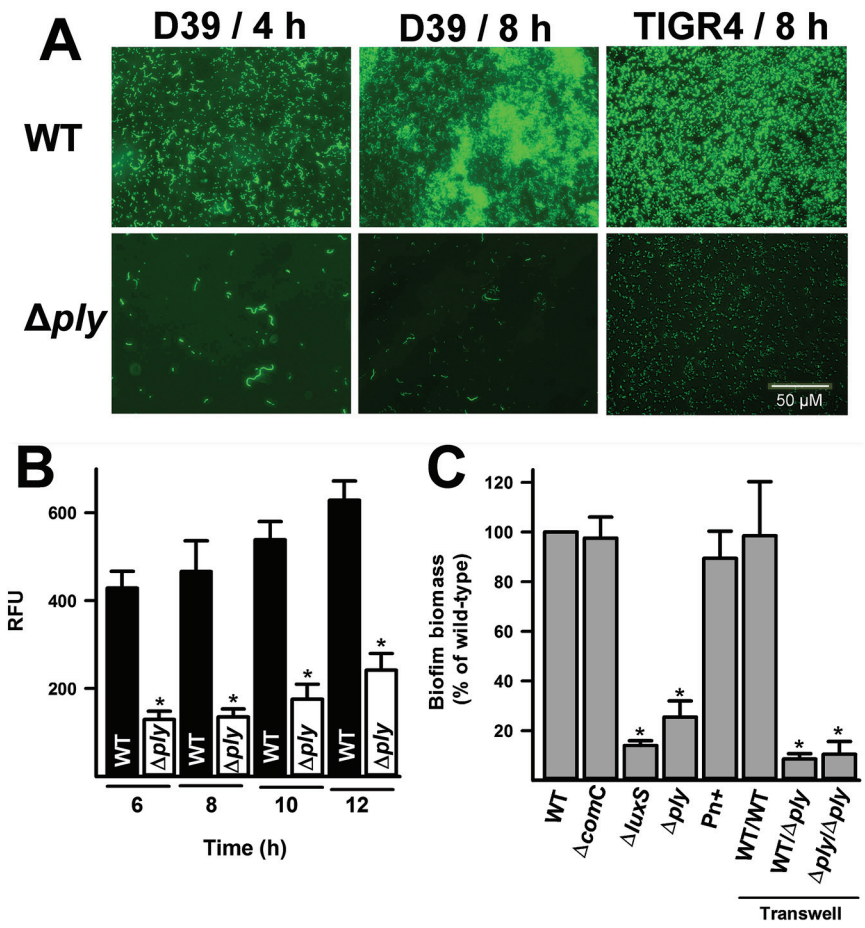

FIG 3 Ply knockout mutants form inferior biofilms on polystyrene at early time points. (A) GFP-expressing D39, D39Δ*ply*, AC2394 (TIGR4), and AC4037 (TIGR4Δ*ply*) were incubated on glass slides for 4 or 8 h, and biofilms were imaged with fluorescence microscopy. (B) Wild-type D39 and D39Δ*ply* biofilm biomasses on polystyrene plates at 6, 8, 10, and 12 h were quantified using a polyclonal FITC-conjugated anti-pneumococcal antibody. Asterisks indicate *P* values of <0.05. (C) Biofilm biomass of D39Δ*comC*, D39Δ*luxS*, D39Δ*ply*, and the complemented strain Pn+ (13) after 8 h of incubation. In addition, biofilm biomass formed on the bottom of the well of Transwell experiments with the wild type above and below, the wild type above and the *ply* mutant below, and the *ply* mutant above and below the barrier, after 10 h of incubation. Values from both the 8-h single-well experiments and 10-h Transwell experiments are expressed as percentages of the biofilm biomass of wild-type D39 at the respective time points. Error bars indicate standard errors of the means, and asterisks indicate *P* values of <0.01.

strains at 4 and 8 h (Fig. 3A). When absolute biofilm biomass was examined using a fluorescein isothiocyanate (FITC)-conjugated antipneumococcal antibody, we found that D39Δ*ply* produced significantly less biomass than the wild type (WT) at 6, 8, 10, and 12 h ($P < 0.05$; Fig. 3B). While a *comC* knockout mutant formed wild-type levels of biofilm biomass on abiotic surfaces, the *luxS* and *ply* knockout mutants formed significantly less biofilm biomass than the wild type ($P < 0.01$) (Fig. 3C). Similar results were obtained when biofilm assays were conducted using polystyrene substrates and Dulbecco's modified Eagle medium (DMEM) (data not shown). As a control, we examined the previously characterized complemented *ply* mutant Pn+ (13) and found that its ability to form biofilms did not differ significantly from that of the wild type (Fig. 3C).

To ascertain whether Ply released into the medium could be sufficient to restore biofilm formation capability to cells lacking endogenous Ply, we conducted experiments using Transwell permeable supports to separate strains of bacteria while allowing the free flow of nutrients and proteins. We grew three combinations of strains in wells with Transwell supports (given in the format top/bottom), WT/WT, WT/Δ*ply* mutant, and Δ*ply* mutant/Δ*ply* mutant. These wells were incubated at 37°C for 10 h, and biofilms on the bottom of the wells were quantified using GFP fluorescence. We found that the Δ*ply* strain with wild-type D39 above the Transwell barrier grew no more biofilms than the Δ*ply* strain with Δ*ply* organisms above the Transwell barrier (Fig. 3C).

The pneumolysin deficient mutant forms comparable biofilm biomass by 24 h, and cellular autolysis is delayed. Quantification of biofilms formed at 18 and 24 h using a fluorescently conjugated antipneumococcal antibody revealed that comparable biofilm biomass was found in wild-type and Δ*ply* strains (Fig. 4A). However, when biofilms were resuspended in phosphate-buffered saline (PBS) and plated on blood agar plates (BAPs), we found that more CFUs were recoverable from the wild-type strain at 8 h and 18 h postinoculation, but at 24 h postinoculation, there were no CFUs recoverable from wild-type D39 biofilms, while D39Δ*ply* and D39Δ*luxS* biofilms still yielded ~1×10^7 CFU/ml (Fig. 4B). Fluorescence microscopy of GFP-expressing D39 and D39Δ*ply* at 24 h revealed that the Δ*ply* strain was more metabolically active (as evidenced by expression of GFP) than the wild-type strain (Fig. 4C). Electron microscopy images directly illustrated pneumococcal autolysis; while wild-type D39 cells in 8-h biofilms contained electron-dense material, wild-type D39 cells in 24-h biofilms have disrupted cellular membranes and exhibit an absence of electron-dense material (Fig. 4D). TEM of the *ply* knockout mutant demonstrated healthy electron-dense cells at both 8 h and 24 h and also showed more surface-associated polysaccharide than in the wild type at 8 h (Fig. 4D).

Ply-deficient D39 forms less biofilm than the wild type on human cell line substrates. To verify that pneumolysin is necessary for early biofilm formation under more physiologically relevant conditions, we examined biofilm formation and *ply* expression in biofilms grown on human cell substrates under static and continuous-flow conditions. When biofilm formation was assessed using an A549 human lung cell substrate in static growth conditions, we observed that wild-type D39 formed confluent biofilms (Fig. 5A), while D39Δ*ply* formed very little biofilm (Fig. 5B). Quantitatively, the biofilm biomass of D39Δ*ply* was significantly less than that of the wild type 6 h ($P < 0.05$) and 8 h ($P < 0.01$) postinoculation (Fig. 5C). In addition, when the strains

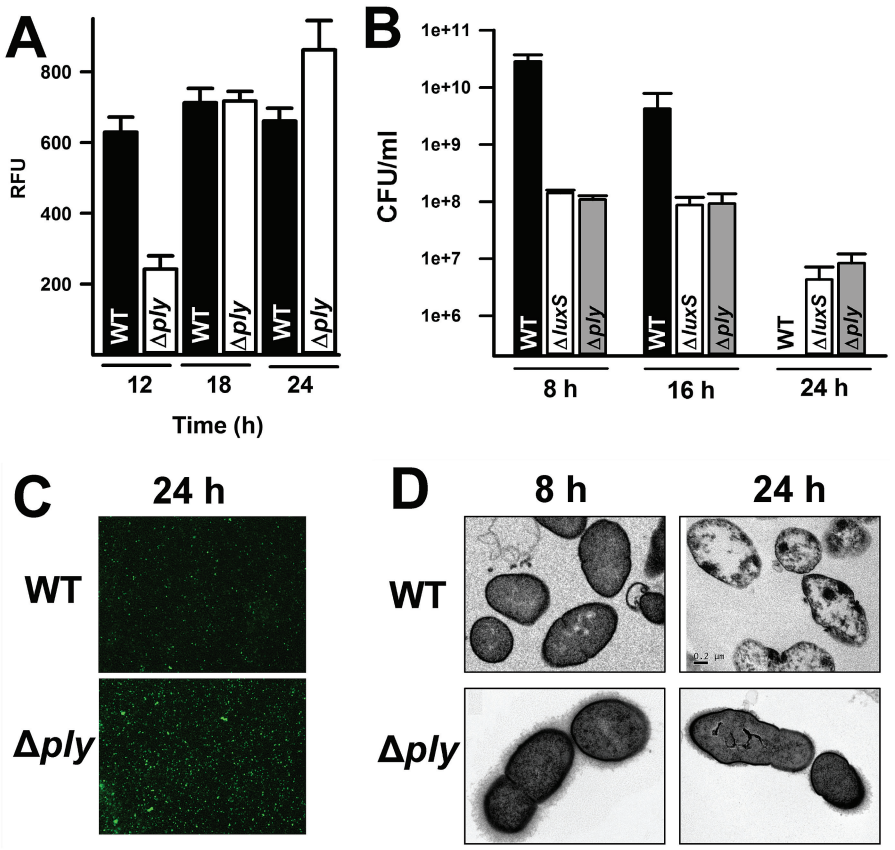

FIG 4 Ply-deficient D39 biofilm formation is comparable to that of the wild type by 24 h, but cellular autolysis is delayed. (A) Biofilm biomasses of D39 and D39Δ*ply* grown on polystyrene for 12, 18, and 24 h, quantified using a FITC-conjugated antipneumococcal antibody. (B) Biofilms formed by D39, D39Δ*luxS*, and D39Δ*ply* on polystyrene after 8, 16, or 24 h of incubation were resuspended in 1 ml of PBS and plated on BAP to estimate CFU. The limit of detection of this assay was 10 CFU/ml. (C) Fluorescence microscopy of GFP-expressing D39 and D39Δ*ply* confirms that the number of enzymatically active cells is greater in D39Δ*ply* biofilms than in wild-type biofilms following 24 h of static incubation. (D) Transmission electron microscopy of wild-type D39 and the Δ*ply* mutant grown on A549 cells demonstrates healthy D39 at 8 h and autolyzed cells at 24 h and healthy Δ*ply* cells at both 8 and 24 h. Error bars indicate standard errors of the means.

were grown on top of Detroit 562 pharyngeal cells for 8 h, we found that D39Δ*ply* and D39Δ*luxS* formed significantly less biofilm biomass than the wild type ($P < 0.01$) (Fig. 5D).

To better simulate *in vivo* conditions of pneumococcal biofilm growth, we grew D39 biofilms on an A549 substrate in a continuous flow bioreactor previously described (27). Confocal microscopy studies demonstrated that Ply coated the bacterial cell wall, with the top section showing pneumococcal chains surrounded by Ply (Fig. 6A) and a middle section showing abundant localization of Ply within aggregated bacteria (Fig. 6B). In relation to the log-phase planktonic inoculum, *ply* expression was upregulated ~6-fold in cells grown on immobilized A549 under static conditions for 8 h, ~2-fold in biofilms grown for 8 h in a bioreactor, and ~6-fold in biofilms grown for 24 h in a bioreactor (Fig. 6C).

Pneumococcal hemolytic activity is not essential for biofilm formation. To examine whether the biofilm formation function of pneumolysin was related to its hemolytic function, we examined the biofilm formation capability of serotype 1 strains belonging to sequence type (ST) 306 that produce a variant of pneumolysin with minimal hemolytic activity (28). Although Western blot analysis confirmed expression of Ply in the serotype 1 strains (see Fig. S4 in the supplemental material), hemolytic activity assays demonstrated the absence of hemolytic activity in D39Δ*ply* and the serotype 1 isolates CDC_881, CDC_1403, and CDC_4829 (Fig. 7A). However, these three serotype 1 strains displayed no statistically significant difference in biofilm biomass at 8 h compared to wild-type D39 (Fig. 7B). Biofilm formation capacity is known to vary markedly between pneumococcal strains. Thus, to ensure that the different genetic background of the serotype 1 strains did not affect the experiment, we constructed Ply306, a D39 derivative expressing the nonhemolytic *ply* allele from ST 306, using methods described previously (29). We found that the biofilm biomass formed by the Ply306 D39 strain did not differ significantly from that of wild-type D39 (Fig. 7B). Taken together, these results suggest that Ply's role in early biofilm formation is independent of hemolytic activity.

As pneumococcal biofilms are present in the nasopharynx with no apparent epithelial damage, the incorporation of Ply into the biofilm matrix may interfere with its hemolytic and cytotoxic activity. We therefore examined the hemolytic activity of wild-type D39 harvested from planktonic cultures in comparison to wild-type D39 harvested from biofilms. While D39 harvested from planktonic cultures maintained constant hemolytic activity over time (Fig. 7C and D), the hemolytic activity of D39 in biofilms

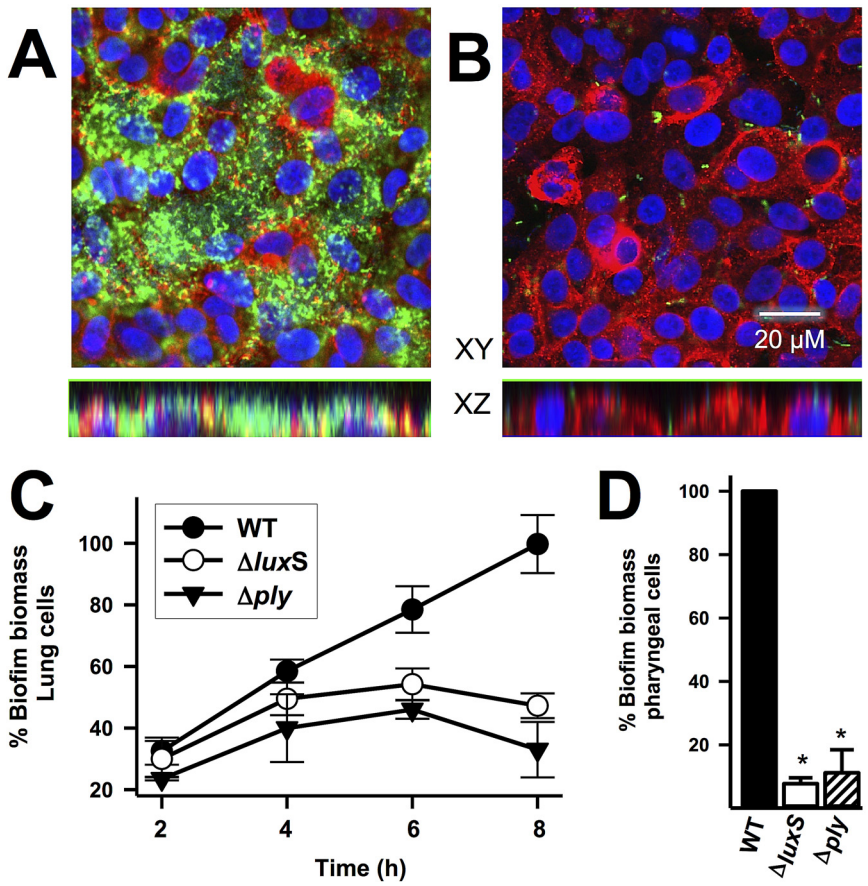

FIG 5 Ply-deficient D39 forms inferior biofilms when grown in static conditions on human lung cells. Wild-type D39 (A) and D39Δ*ply* (B) biofilms were grown under static conditions for 8 h on A549 human lung cell substrates. GFP-expressing bacteria are green, eukaryotic nuclei are blue, and eukaryotic membranes are red. (C) Wild-type D39, D39Δ*luxS*, and D39Δ*ply* were grown on human lung A549 cells under static conditions for 2, 4, 6, and 8 h, and biofilm biomass was quantified using GFP fluorescence. The amount of biofilm biomass is shown as a percentage of that formed by wild-type D39 at 8 h. At 6 and 8 h postinoculation, wild-type D39 formed significantly more biofilm biomass than D39Δ*luxS* or D39Δ*ply* ($P < 0.05$). (D) D39Δ*luxS* and D39Δ*ply* form significantly less biofilm than wild-type D39 when grown on Detroit 562 human pharyngeal cells for 8 h under static conditions. Error bars indicate standard errors of the means, and asterisks indicate *P* values of <0.01.

decreased from 128 hemolytic units (HU)/mg at 6 h postinoculation (Fig. 7C) to 64 HU/mg 8 h postinoculation (data not shown) and further to 32 HU/mg at 10 h postinoculation (Fig. 7D). This difference suggests that incorporation of pneumococcal cells into biofilms is correlated with a decrease in hemolytic activity.

DISCUSSION

This study is the first to demonstrate that pneumolysin is essential for the production of early pneumococcal biofilms. Not only was Ply expressed in pneumococcal biofilms produced under static and continuous-flow conditions on abiotic and human cell substrates, but Ply knockout mutants produced significantly less biofilm biomass than the wild type at early time points. Early aggregates of pneumococci were the first to express pneumolysin, and expression peaked with maximal biofilm formation at approximately 8 to 10 h postinoculation. Incorporation of cells into biofilms led to a decrease in hemolytic activity, but the hemolytic function of Ply appears to be separate from its role in biofilm formation. In total, we have demonstrated that pneumolysin has a previously unrecognized role, key in the early stages of the biofilm formation process.

Previous studies have alluded to a connection between pneumolysin and biofilm formation. Most evidence has been circumstantial, demonstrating that biofilm formation results in changes in *ply* expression. In 2006, Oggioni et al. reported extensive regulatory differences between planktonic and sessile phases, including the finding that in comparison to mid-exponential-phase liquid cultures, pneumococcal cells on agar and in biofilms expressed 100-fold and 5-fold less *ply*, respectively (30). Lizcano et al. concluded that pneumolysin was not important in biofilm formation in TIGR4; however their study only examined biofilm biomass by measuring crystal violet staining at 18 h postinoculation (31). Our results indicate that after 18 h of growth, cells in wild-type biofilms may have already begun to undergo autolysis, while the Ply knockout mutant continues to form more biofilm (7, 32). By examining biofilm formation of wild-type strains and isogenic mutants using various growth conditions, multiple substrates, and a variety of time points, we have shown that there is an important role for pneumolysin in the early stages of pneumococcal biofilm development.

Confocal and electron microscopy localized pneumolysin to the pneumococcal cell surface and extracellular matrix, suggesting a linking role for this protein during the aggregation phase of biofilm formation. While altered degradation of GFP may be responsible for the difference in autolysis witnessed by fluorescence, our CFU measurements and TEM results clearly demonstrate that the *ply* knockout mutant has delayed autolysis. This may be a function of metabolic changes, perhaps resulting from altered proximity to other bacterial cells. Previous studies have indicated that presence of a capsule impairs pneumococcal biofilm formation (33, 34) and that genes in the capsule operon are downregulated during biofilm formation (35). The polysaccharide halo surrounding the *ply* knockout cells imaged by TEM is consistent with altered capsular regulation, but further studies are needed to understand the role of capsular expression in pneumococcal biofilm formation.

Pneumolysin has been recognized as a virulence determinant for decades (36), and animal and human studies have indicated that the hemolytic activity of pneumolysin is largely responsible for pneumococcal virulence (37). However, the amount of hemolytic activity necessary for virulence is reportedly just 0.1% of the wild-type levels (13). Nevertheless, it was surprising when Kirkham et al. reported the isolation of nonhemolytic serotype 1 strains from invasive pneumococcal disease (28). This result led

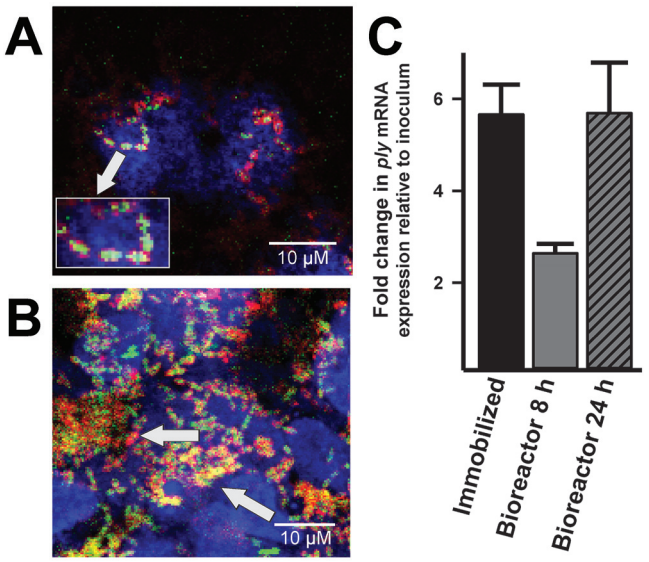

FIG 6 Pneumolysin is expressed in biofilms produced on human lung cells in a continuous-flow bioreactor. (A) The optical top section from a bioreactor with wild-type D39 biofilm cells on an A549 human cell substrate after 8 h of growth. Cells and biofilms were fixed, nuclei were fluorescently stained with TO-PRO-3 (blue), and Ply was stained with an anti-Ply antibody (red). Arrows indicate GFP-expressing pneumococci (green) surrounded by Ply, enlarged in the inset. (B) The middle section from the same 8-h bioreactor demonstrates abundant Ply expressed within pneumococcal biofilm aggregates grown in this model system. (C) Reverse transcription and qPCR of RNA extracted from biofilms grown on immobilized cells in static culture for 8 h or in a continuous-flow bioreactor for 8 or 24 h demonstrate that *ply* is upregulated relative to the inoculum when the bacteria are grown on A549 cells. Error bars indicate standard errors of the means.

those authors to speculate that an immune activation function of pneumolysin may contribute to virulence; this hypothesis is supported by the findings of Malley et al. showing that pneumolysin induces a substantial immune response by macrophages (17). The results of our study raise the possibility that pneumolysin's contribution to pneumococcal virulence may be partially attributed to its role in biofilm formation. At the same time, our finding that pneumococcal hemolytic activity of cells decreases as biofilms are formed may indicate that incorporation of cells into the biofilm matrix may mask the hemolytic epitope and prevent pneumolysin from provoking a clearing immune response during carriage.

Recently we demonstrated that LuxS/AI-2 regulates early pneumococcal biofilm formation (7, 8) and observed that a *luxS* null mutant expressed lower mRNA levels of the pneumolysin gene than the wild type. In a follow-up study, we demonstrated that both the LuxS/AI-2 and Com quorum-sensing systems regulate biofilm production in a bioreactor with living cultures of human respiratory cells (27). Our finding that pneumolysin is downregulated in a *luxS* knockout mutant but not in a *comC* knockout mutant appears to indicate that pneumolysin is predominantly under the regulatory control of the LuxS/AI-2 system. From these results we can hypothesize that LuxS-regulated pneumolysin plays a critical role in early aggregation, while other factors regulated by Com contribute to biofilm maturation. The components of biofilm assembly and maturation, and the regulation of those components, are a subject in need of further study.

Our results suggest that pneumolysin directly contributes to early aggregation of pneumococcal cells into early biofilms. Given that pneumolysin is an important candidate antigen for the development of a serotype-independent vaccine (19–21, 38, 39), our

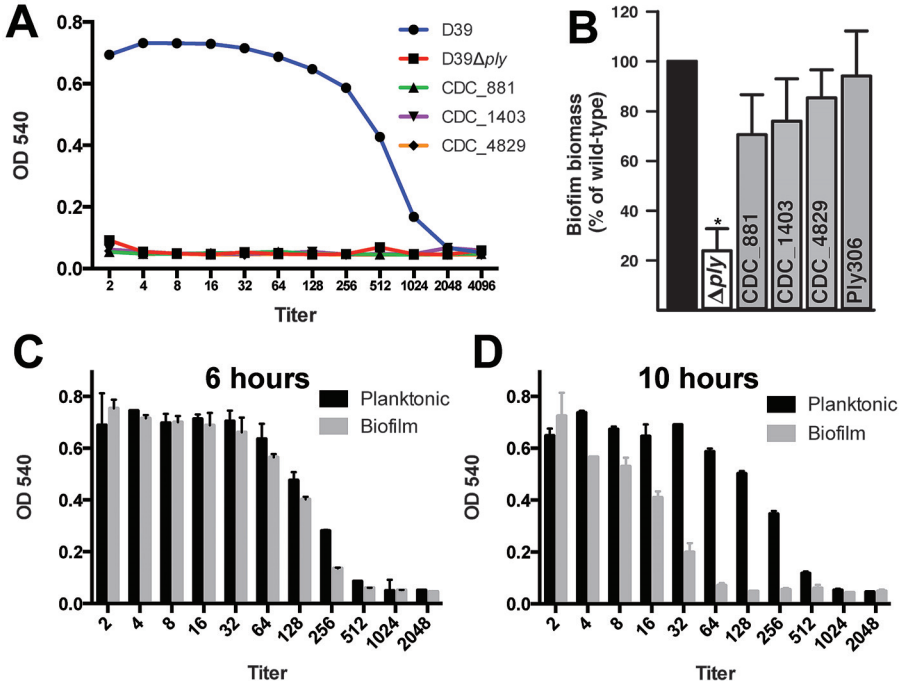

FIG 7 Hemolytic activity and biofilm phenotypes. (A) D39, D39Δ*ply*, and three serotype 1 isolates were examined for hemolytic activity. Wild-type D39 possessed hemolytic activity, while all other strains examined had almost none. (B) When biofilm formation capability was assessed, CDC_881, CDC_1403, CDC 4829, and Ply306 exhibited biofilm biomasses similar to that of wild-type D39. (C) Wild-type D39 cells harvested from planktonic and biofilm cultures assayed for hemolytic activity did not differ in hemolytic activity at 6 h postinoculation. (D) Planktonic and biofilm cultures of D39 harvested 10 h postinoculation demonstrate a marked difference in hemolytic activity. Error bars indicate standard deviations, and the asterisk indicates a P value of <0.01.

characterization of pneumolysin's role in biofilm formation has important implications. Carriage of the pneumococcus is a necessary precursor to pneumococcal diseases (40) and if Ply is routinely expressed in nasopharyngeal biofilms, its potential as a vaccine antigen is more easily understood. These results highlight the urgent need for further exploration of pneumolysin and the immune response against it, using both *in vivo* and *in vitro* models of biofilm formation.

MATERIALS AND METHODS

Strains and bacterial culture methods. The *S. pneumoniae* reference and derivative strains used in this study are listed in Table 1. Strains were cultured on Trypticase soy agar BAPs or in Todd-Hewitt broth containing 0.5% (wt/vol) yeast extract (THY). When biofilm formation was visualized or quantified using GFP-expressing strains, 2% (wt/vol) maltose was added to the culture medium. Inocula for all biofilm assays were prepared using growth on an overnight BAP to prepare a cell suspension in THY broth at an optical density at 600 nm (OD_{600}) of 0.05. This suspension was incubated at 37°C in a 5% CO_2 atmosphere until the culture reached an OD_{600} of 0.2 to 0.3 (early log phase); glycerol was added to a final concentration of 10% (vol/vol), and the suspension was stored at −80°C until used.

Growth of biofilms on abiotic and biotic surfaces. For experiments conducted on abiotic surfaces, 24-well Costar polystyrene plates (Corning, Tewksbury, MA) were used for quantification experiments, and 8-well Lab-Tek II glass chamber slides (Thermo, Fisher Scientific, Rockford, IL) were used for visualization experiments. Wells or chambers were filled with THY medium, inoculated 1:10 with inocula prepared as described above, and incubated at 37°C for various lengths of time. When indicated, experiments used Transwell permeable supports (Corning, Tewksbury, MA) with 0.4-μm pores to separate strains of bacteria within wells of 24-well plates while allowing the free flow of nutrients and secreted proteins.

To simulate the environment in the human respiratory tract, a human cell line substrate was employed, in both static and continuous-flow cultures, as recently described (27). Briefly, human-derived lung A549 cells (ATCC CCL-185) or human-derived pharyngeal Detroit 562 cells (ATCC CCL-198) were grown on polystyrene plates or Snapwell filters (Corning, Tewksbury, MA) until confluent (4 to 5 days). For static experiments, human cells were fixed with 2% paraformaldehyde (Sigma) for 15 min. Following several washes with PBS, immobilized human cells were inoculated with prepared bacterial inocula (~7×10^5 CFU/ml) and incubated in DMEM at 37°C for various times. For continuous-flow experiments, confluent cells on Snapwell filters were inoculated as detailed above and immediately placed in a sterile vertical diffusion chamber (27). Both basolateral and apical sides (inner chamber) were perfused with sterile DMEM with no antibiotics using a Master Flex L/S precision pump system (Cole-Parmer, Vernon, IL) at a low flow rate (0.20 ml/min). Bioreactor chambers containing *S. pneumoniae* and lung cells were incubated at 37°C in a sterile environment. At the end of the incubation period, inserts containing biofilms were removed, and biomass was analyzed qualitatively and quantitatively.

Visualizing pneumococcal biofilms. When GFP-expressing strains were used, biofilms on microtiter plates were washed with PBS and visualized by fluorescence microscopy, or biofilms produced on 8-chamber slides were washed with PBS, fixed with 2% paraformaldehyde, and mounted with Vectashield (Vector Laboratories, Burlingame, CA), and fluorescence was visualized with an inverted Evos FL microscope (Advanced Microscopy Group, Carlsbad, CA) or confocal microscopy. When non-GFP-expressing strains were used, biofilms were fixed with 2% paraformaldehyde (Sigma-Aldrich, St. Louis, MO) for 15 min, washed with PBS, blocked with 2% bovine serum albumin, and stained for 1 h at room temperature with a polyclonal anti-*S. pneumoniae* antibody (~40 μg/ml) coupled to fluorescein isothiocyanate (FITC; ViroStat, Portland, ME). Where indicated, Ply was detected using 2.0 μg/ml unconjugated mouse monoclonal anti-Ply antibody (Santa Cruz Biotechnology, Santa Cruz, CA), followed by an Alexa Fluor 568 goat anti-mouse IgG secondary antibody (Molecular Probes, Invitrogen, Carlsbad, CA). For preparations from the human cell bioreactor system, sialic acid residues present on the plasma membranes were stained with 5 μg/ml wheat germ agglutinin conjugated with Alexa Fluor 555 (Molecular Probes, Invitrogen, Carlsbad, CA) for 30 min (41), and nucleic acids were stained with TO-PRO-3 (1 μM), a carbocyanine monomer nucleic acid stain (Molecular Probes, Invitrogen, Carlsbad, CA) for 15 min. Finally, preparations were washed three times with PBS, mounted with Vectashield mounting medium (Vector Laboratories, Burlingame, CA), and analyzed with a Zeiss LSM510 confocal microscope. Confocal images were analyzed with an LSM image browser, version 4.0.2.121.

For immunogold localization of Ply, 8-h biofilms grown on top of A549 lung cells were fixed with either 2 or 4% paraformaldehyde (PFA) in 0.1 M phosphate buffer (PB) overnight at 4°C. Cells were then washed and treated with 0.05% Triton X-100 for 10 min before blocking with PBS containing 5% bovine serum albumin (BSA) and 0.1% cold-water-fish gelatin. Mouse anti-Ply primary antibody was diluted to 8 μg/ml in PBS containing 0.1% acetylated BSA for overnight incubation. After washes, cells were incubated overnight with ultrasmall-colloidal-gold-conjugated goat anti-mouse IgG secondary antibody (Aurion, Wageningen, the Netherlands), followed by washes and postfixation in 2.5% buffered glutaraldehyde. Silver enhancement of ultrasmall gold particles was carried out using R-gent SE-EM silver enhancement kit (Aurion, Wageningen, the Netherlands) following the manufacturer's instruction. Cells were then fixed with 0.5% osmium tetroxide, dehydrated, and embedded in Eponate 12 resin. Ultrathin sections were counterstained with 5% uranyl acetate and 2% lead citrate and examined on a JEOL JEM-1400 transmission electron microscope (JEOL Ltd., Japan) equipped with a Gatan UltraScan US1000 charge-coupled device (CCD) camera (Gatan, Inc., Pleasanton, CA).

Quantification of biofilm biomass. Biofilm biomass was quantified by fluorescence methods as previously described (7, 27) or by serial dilution followed by plating to obtain cell counts (CFU/ml). For GFP-expressing strains and biofilms stained with a FITC-conjugated antibody, arbitrary relative fluorescence units (RFU) were obtained using a Victor X3 multilabel plate reader (PerkinElmer, Waltham, MA). The number of arbitrary fluorescence units of wild-type D39 was set to a biofilm biomass of 100% and used to calculate the biofilm biomass percentages of all of the other *S. pneumoniae* strains tested and those at different time points. Results of repeated experiments were plotted using GraphPad Prism or SigmaPlot and examined for statistical significance with two-tailed *t* tests for normal data and Mann-Whitney *U* tests for nonparametric data.

Western blot assays. To compare the expression of Ply in biofilm and planktonic cells, bacterial cells were treated with the B-PER bacterial protein extraction reagent (Thermo, Fisher Scientific, Rockford, IL) according to the manufacturer's protocol and quantified using the Bradford protein assay (42). A 5-μg portion of extracted protein was loaded into each well on a 12% polyacrylamide gel, subjected to SDS-PAGE, and transferred onto a nitrocellulose membrane. Those membranes were blocked with PBS with 0.05% (vol/vol) Tween 20 and 5% (wt/vol) nonfat dry milk for 1 h and then probed with a 1:200 dilution (final concentration, 0.5 μg/ml) of mouse anti-Ply monoclonal antibody (Santa Cruz Biotechnology, Santa Cruz, CA) (43). Bound antibody was detected with a horseradish peroxidase-conjugated secondary anti-mouse antibody diluted 1:10,000 and addition of Pierce ECL Western blotting substrate (Thermo, Fisher Scientific, Rockford, IL).

Construction of D39 derivatives with *ply* knocked out or modified. A *ply* knockout mutant was generated by PCR ligation mutagenesis as previously described (44) (see Fig. S1 in the supplemental material). Briefly, the construct was generated by PCR amplification of a 5′ segment of the *ply* gene with primers HPL1 and HPL2 and a 3′ segment with primers HPL5 and HPL6. Primers HPL3 and HPL4 were used to amplify the *ermB* gene, encoding erythromycin resistance, and to add XbaI and

TABLE 2 Primers used in this study

Primer	Target gene	Sequence[a]	RE site	PCR product size (bp)
HPL1L	SPD1728-*ply*	TTGGCGACAAGCATTTTGTA		800
HPL2R	*ply*-SPD1728	CAGTCTAGACCACTACGAGAAGTGCTCCA	XbaI	
HPL3L	*ermB*	CAGTCTAGAAAAAATTTGTAATTAAGAAGGAGT	XbaI	796
HPL4R	*ermB*	CAGCTCGAGCCAAATTTACAAAAGCGACTCA	XhoI	
HPL5L	*ply*-flank	CAGCTCGAGCTTTAAAAGGGAATGTTCGTAATCTCT	XhoI	800
HPL6R	Flank-*ply*	GCGACAAAAACAATCATACTGC		
JVS35L	16S rRNA	AACCAAGTAACTTTGAAAGAAGAC		126
JVS36R	16S rRNA	AAATTTAGAATCGTGGAATTTTT		
JVS59L	*ply*	TGAGACTAAGGTTACAGCTTACAG		225
JVS60R	*ply*	CTAATTTTGACAGAGAGATTACGA		
luxS-L	*luxS*	ACATCATCTCCAATTATGATATTC		257
luxS-R	*luxS*	GACATCTTCCCAAGTAGTAGTTTC		

[a] Underlining indicates the restriction enzyme (RE) site used for cloning.

XhoI restriction sites to the ends (7). The 5′ and 3′ segments were ligated to the gene encoding erythromycin resistance using T4 DNA ligase, and the cassette was generated by amplification with primers HPL1 and HPL6. A 100-ng portion of the cassette was then transformed into competent D39 cells, and the SPJV14 (D39Δ*ply*) recombinants were selected for on BAP containing 0.5 μg/ml of erythromycin. Knockouts were confirmed by PCR (see Fig. S1 in the supplemental material), sequencing (data not shown), and Western blotting (see Fig. S4 in the supplemental material). A derivative of D39 expressing the nonhemolytic *ply* allele from an *S. pneumoniae* type 1 ST 306 strain was constructed by allelic replacement using an analogous protocol and the primers employed for construction of a derivative expressing the ply_{4496} allele, which has significantly less hemolytic activity (29).

Hemolytic activity assay. Pneumococcal cells were prepared for assay by growth in THY to mid-log phase (OD_{600}, 0.3 to 0.4) and 10× concentration before resuspension in PBS. Bacterial cells were lysed with a 10-min incubation at 37°C in 0.1% sodium deoxycholate solution, and then protein was quantified using the Bradford assay. Sheep red blood cells (RBCs) were washed three times using PBS. RBCs (2 ml) were added to 32 ml PBS and 50 μl β-mercaptoethanol to make a 3% RBC preparation. Serial 2-fold dilutions of 17 μg of each protein preparation were made in PBS in microtiter plates before addition of 50 μl of the 3% RBC preparation and incubation for 30 min at 37°C. Unlysed RBCs were pelleted by centrifugation, and supernatant was transferred to a new microtiter plate for measurement at A_{540}. A_{540} values were plotted against the dilution factor. Hemolytic units are defined as the lysate dilution factor when hemolysis is 50% of that of wild-type D39.

Gene expression studies. Suspensions of biofilm cells or planktonic cells were combined with an equal volume of RNA Protect (Qiagen Inc., Valencia, CA). Total RNA was extracted with an RNeasy minikit (Qiagen Inc., Valencia, CA) and treated with 2 U of DNase I (Promega, Madison, WI) as previously described (7). The integrity of RNA preparations and the concentrations of samples were assessed using a NanoDrop ND-1000 spectrophotometer (Thermo, Fisher Scientific, Wilmington, DE). Total RNA was reverse transcribed into cDNA using an iScript cDNA synthesis kit (Bio-Rad, Hercules, CA), using the manufacturer's instructions. Quantitative PCR (qPCR) was performed with generated cDNA using SYBR green (Bio-Rad, Hercules, CA) and a CFX96 real-time PCR detection system (Bio-Rad, Hercules, CA). qPCRs were performed in duplicate with 30 ng of total RNA, a 250 nM concentration of the primers JVS59L and JVS60R to quantify *ply* transcripts (Table 2), and the following conditions: 1 cycle of 95°C for 3 min, 40 cycles of 95°C for 30 s and 55°C for 30 s, and 1 cycle of 72°C for 1 min. Melting curves were acquired on SYBR green channel from 65°C to 95°C with 0.5°C increments. Relative quantities of mRNA expression were normalized to the constitutive expression of the housekeeping 16S rRNA gene (7) calculated by the comparative $2(-\Delta\Delta C_T)$ method (45). Error bars in the figures represent the standard errors of the means calculated using data from three independent experiments.

SUPPLEMENTAL MATERIAL

Supplemental material for this article may be found at http://mbio.asm.org/lookup/suppl/doi:10.1128/mBio.00655-13/-/DCSupplemental.

Figure S1, EPS file, 1.2 MB.
Figure S2, EPS file, 14.8 MB.
Figure S3, EPS file, 1 MB.
Figure S4, EPS file, 1.2 MB.

ACKNOWLEDGMENTS

This work was supported in part by URC/ACTSI 16407 PHS grant UL1 RR025008 to J.E.V. from the Clinical and Translational Science Award program, NIH, National Center for Research Resources and program grant 565526 from the National Health and Medical Research Council (NHMRC) of Australia to J.C.P. J.R.S. acknowledges financial support from the Molecules to Mankind Program at Emory's Laney Graduate School and the Medical Scientist Training Program at Emory University School of Medicine.

We thank Lesley McGee of the Centers for Disease Control for providing serotype 1 strains, Andrew Camilli of Tufts University for providing TIGR4 derivatives, and Manuel Espinosa of Centro de Investigaciones Biologicas, Madrid, Spain, for his gift of plasmid pMV158GFP.

REFERENCES

1. **O'Brien KL, Wolfson LJ, Watt JP, Henkle E, Deloria-Knoll M, McCall N, Lee E, Mulholland K, Levine OS, Cherian T, Hib and Pneumococcal Global Burden of Disease Study Team.** 2009. Burden of disease caused by *Streptococcus pneumoniae* in children younger than 5 years: global estimates. Lancet **374:**893–902.
2. **Shak JR, Vidal JE, Klugman KP.** 2013. Influence of bacterial interactions on pneumococcal colonization of the nasopharynx. Trends Microbiol. **21:**129–135.
3. **Domenech M, García E, Moscoso M.** 2012. Biofilm formation in *Streptococcus pneumoniae*. Microb. Biotechnol. **5:**455–465.
4. **Hall-Stoodley L, Hu FZ, Gieseke A, Nistico L, Nguyen D, Hayes J, Forbes M, Greenberg DP, Dice B, Burrows A, Wackym PA, Stoodley P, Post JC, Ehrlich GD, Kerschner JE.** 2006. Direct detection of bacterial biofilms on the middle-ear mucosa of children with chronic otitis media. JAMA **296:**202–211.
5. **Reid SD, Hong W, Dew KE, Winn DR, Pang B, Watt J, Glover DT, Hollingshead SK, Swords WE.** 2009. *Streptococcus pneumoniae* forms surface-attached communities in the middle ear of experimentally infected chinchillas. J. Infect. Dis. **199:**786–794.
6. **Weimer KE, Armbruster CE, Juneau RA, Hong W, Pang B, Swords WE.** 2010. Coinfection with *Haemophilus influenzae* promotes pneumococcal biofilm formation during experimental otitis media and impedes the progression of pneumococcal disease. J. Infect. Dis. **202:**1068–1075.

7. **Vidal JE, Ludewick HP, Kunkel RM, Zähner D, Klugman KP.** 2011. The LuxS-dependent quorum-sensing system regulates early biofilm formation by *Streptococcus pneumoniae* strain D39. Infect. Immun. **79:** 4050–4060.
8. **Trappetti C, Potter AJ, Paton AW, Oggioni MR, Paton JC.** 2011. LuxS mediates iron-dependent biofilm formation, competence, and fratricide in *Streptococcus pneumoniae*. Infect. Immun. **79:**4550–4558.
9. **Paton JC, Andrew PW, Boulnois GJ, Mitchell TJ.** 1993. Molecular analysis of the pathogenicity of *Streptococcus pneumoniae*: the role of pneumococcal proteins. Annu. Rev. Microbiol. **47:**89–115.
10. **Hirst RA, Gosai B, Rutman A, Guerin CJ, Nicotera P, Andrew PW, O'Callaghan C.** 2008. *Streptococcus pneumoniae* deficient in pneumolysin or autolysin has reduced virulence in meningitis. J. Infect. Dis. **197:** 744–751.
11. **Price KE, Camilli A.** 2009. Pneumolysin localizes to the cell wall of *Streptococcus pneumoniae*. J. Bacteriol. **191:**2163–2168.
12. **Alouf JE.** 2000. Cholesterol-binding cytolytic protein toxins. Int. J. Med. Microbiol. **290:**351–356.
13. **Berry AM, Alexander JE, Mitchell TJ, Andrew PW, Hansman D, Paton JC.** 1995. Effect of defined point mutations in the pneumolysin gene on the virulence of *Streptococcus pneumoniae*. Infect. Immun. **63:**1969–1974.
14. **Kaur R, Casey JR, Pichichero ME.** 2011. Serum antibody response to five *Streptococcus pneumoniae* proteins during acute otitis media in otitis-prone and non-otitis-prone children. Pediatr. Infect. Dis. J. **30:**645–650.
15. **Simell B, Korkeila M, Pursiainen H, Kilpi TM, Käyhty H.** 2001. Pneumococcal carriage and otitis media induce salivary antibodies to pneumococcal surface adhesin a, pneumolysin, and pneumococcal surface protein a in children. J. Infect. Dis. **183:**887–896.
16. **Rapola S, Kilpi T, Lahdenkari M, Mäkelä PH, Käyhty H.** 2001. Antibody response to the pneumococcal proteins pneumococcal surface adhesin A and pneumolysin in children with acute otitis media. Pediatr. Infect. Dis. J. **20:**482–487.
17. **Malley R, Henneke P, Morse SC, Cieslewicz MJ, Lipsitch M, Thompson CM, Kurt-Jones E, Paton JC, Wessels MR, Golenbock DT.** 2003. Recognition of pneumolysin by Toll-like receptor 4 confers resistance to pneumococcal infection. Proc. Natl. Acad. Sci. U. S. A. **100:**1966–1971.
18. **Dogan S, Zhang Q, Pridmore AC, Mitchell TJ, Finn A, Murdoch C.** 2011. Pneumolysin-induced CXCL8 production by nasopharyngeal epithelial cells is dependent on calcium flux and MAPK activation via Toll-like receptor 4. Microbes Infect. **13:**65–75.
19. **Malley R, Anderson PW.** 2012. Serotype-independent pneumococcal experimental vaccines that induce cellular as well as humoral immunity. Proc. Natl. Acad. Sci. U. S. A. **109:**3623–3627.
20. **Salha D, Szeto J, Myers L, Claus C, Sheung A, Tang M, Ljutic B, Hanwell D, Ogilvie K, Ming M, Messham B, van den Dobbelsteen G, Hopfer R, Ochs MM, Gallichan S.** 2012. Neutralizing antibodies elicited by a novel detoxified pneumolysin derivative, PlyD1, provide protection against both pneumococcal infection and lung injury. Infect. Immun. **80:** 2212.
21. **Kamtchoua T, Bologa M, Hopfer R, Neveu D, Hu B, Sheng X, Corde N, Pouzet C, Zimmermann G, Gurunathan S.** 2013. Safety and immunogenicity of the pneumococcal pneumolysin derivative PlyD1 in a single-antigen protein vaccine candidate in adults. Vaccine **31:**327–333.
22. **Caiazza NC, O'Toole GA.** 2003. Alpha-toxin is required for biofilm formation by *Staphylococcus aureus*. J. Bacteriol. **185:**3214–3217.
23. **Anderson MJ, Lin YC, Gillman AN, Parks PJ, Schlievert PM, Peterson ML.** 2012. Alpha-toxin promotes *Staphylococcus aureus* mucosal biofilm formation. Front. Cell. Infect. Microbiol. **2:**64.
24. **Allegrucci M, Hu FZ, Shen K, Hayes J, Ehrlich GD, Post JC, Sauer K.** 2006. Phenotypic characterization of *Streptococcus pneumoniae* biofilm development. J. Bacteriol. **188:**2325–2335.
25. **Marks LR, Parameswaran GI, Hakansson AP.** 2012. Pneumococcal interactions with epithelial cells are crucial for optimal biofilm formation and colonization in vitro and in vivo. Infect. Immun. **80:**2744–2760.
26. **Joyce EA, Kawale A, Censini S, Kim CC, Covacci A, Falkow S.** 2004. LuxS is required for persistent pneumococcal carriage and expression of virulence and biosynthesis genes. Infect. Immun. **72:**2964–2975.
27. **Vidal JE, Howery KE, Ludewick HP, Nava P, Klugman KP.** 2013. Quorum-sensing systems LuxS/autoinducer 2 and com regulate *Streptococcus pneumoniae* biofilms in a bioreactor with living cultures of human respiratory cells. Infect. Immun. **81:**1341–1353.
28. **Kirkham LA, Jefferies JM, Kerr AR, Jing Y, Clarke SC, Smith A, Mitchell TJ.** 2006. Identification of invasive serotype 1 pneumococcal isolates that express nonhemolytic pneumolysin. J. Clin. Microbiol. **44:** 151–159.
29. **Harvey RM, Ogunniyi AD, Chen AY, Paton JC.** 2011. Pneumolysin with low hemolytic activity confers an early growth advantage to *Streptococcus pneumoniae* in the blood. Infect. Immun. **79:**4122–4130.
30. **Oggioni MR, Trappetti C, Kadioglu A, Cassone M, Iannelli F, Ricci S, Andrew PW, Pozzi G.** 2006. Switch from planktonic to sessile life: a major event in pneumococcal pathogenesis. Mol. Microbiol. **61:**1196–1210.
31. **Lizcano A, Chin T, Sauer K, Tuomanen EI, Orihuela CJ.** 2010. Early biofilm formation on microtiter plates is not correlated with the invasive disease potential of *Streptococcus pneumoniae*. Microb. Pathog. **48:** 124–130.
32. **Wei H, Håvarstein LS.** 2012. Fratricide is essential for efficient gene transfer between pneumococci in biofilms. Appl. Environ. Microbiol. **78:** 5897–5905.
33. **Moscoso M, García E, López R.** 2006. Biofilm formation by Streptococcus pneumoniae: role of choline, extracellular DNA, and capsular polysaccharide in microbial accretion. J. Bacteriol. **188:**7785–7795.
34. **Qin L, Kida Y, Imamura Y, Kuwano K, Watanabe H.** 2013. Impaired capsular polysaccharide is relevant to enhanced biofilm formation and lower virulence in Streptococcus pneumoniae. J. Infect. Chemother. **19:** 261–271.
35. **Hall-Stoodley L, Nistico L, Sambanthamoorthy K, Dice B, Nguyen D, Mershon WJ, Johnson C, Hu FZ, Stoodley P, Ehrlich GD, Post JC.** 2008. Characterization of biofilm matrix, degradation by DNase treatment and evidence of capsule downregulation in Streptococcus pneumoniae clinical isolates. BMC Microbiol. **8:**173.
36. **Berry AM, Yother J, Briles DE, Hansman D, Paton JC.** 1989. Reduced virulence of a defined pneumolysin-negative mutant of *Streptococcus pneumoniae*. Infect. Immun. **57:**2037–2042.
37. **Marriott HM, Mitchell TJ, Dockrell DH.** 2008. Pneumolysin: a double-edged sword during the host-pathogen interaction. Curr. Mol. Med. **8:**497–509.
38. **Ljutic B, Ochs M, Messham B, Ming M, Dookie A, Harper K, Ausar SF.** 2012. Formulation, stability and immunogenicity of a trivalent pneumococcal protein vaccine formulated with aluminum salt adjuvants. Vaccine **30:**2981–2988.
39. **Mahdi LK, Wang H, Van der Hoek MB, Paton JC, Ogunniyi AD.** 2012. Identification of a novel pneumococcal vaccine antigen preferentially expressed during meningitis in mice. J. Clin. Invest. **122:**2208–2220.
40. **Simell B, Auranen K, Käyhty H, Goldblatt D, Dagan R, O'Brien KL, Pneumococcal Carriage Group.** 2012. The fundamental link between pneumococcal carriage and disease. Expert Rev. Vaccines **11:**841–855.
41. **Wright CS.** 1984. Structural comparison of the two distinct sugar binding sites in wheat germ agglutinin isolectin II. J. Mol. Biol. **178:**91–104.
42. **Bradford MM.** 1976. A rapid and sensitive method for the quantitation of microgram quantities of protein utilizing the principle of protein-dye binding. Anal. Biochem. **72:**248–254.
43. **Fisher DJ, Miyamoto K, Harrison B, Akimoto S, Sarker MR, McClane BA.** 2005. Association of beta2 toxin production with *Clostridium perfringens* type A human gastrointestinal disease isolates carrying a plasmid enterotoxin gene. Mol. Microbiol. **56:**747–762.
44. **Lau PC, Sung CK, Lee JH, Morrison DA, Cvitkovitch DG.** 2002. PCR ligation mutagenesis in transformable streptococci: application and efficiency. J. Microbiol. Methods **49:**193–205.
45. **Livak KJ, Schmittgen TD.** 2001. Analysis of relative gene expression data using real-time quantitative PCR and the $2(-\Delta\Delta C_T)$ method. Methods **25:**402–408.
46. **Avery OT, Macleod CM, McCarty M.** 1944. Studies on the chemical nature of the substance inducing transformation of pneumococcal types: induction of transformation by a desoxyribonucleic acid fraction isolated from pneumococcus type III. J. Exp. Med. **79:**137–158.
47. **Price KE, Greene NG, Camilli A.** 2012. Export requirements of pneumolysin in *Streptococcus pneumoniae*. J. Bacteriol. **194:**3651–3660.
48. **Nieto C, Espinosa M.** 2003. Construction of the mobilizable plasmid pMV158GFP, a derivative of pMV158 that carries the gene encoding the green fluorescent protein. Plasmid **49:**281–285.